Copyright © 1996 Elsevier Science Ltd
Paper No. 567. (quote when citing this article)
Eleventh World Conference on Earthquake Engineering
ISBN: 0 08 042822 3

DEFORMATION CONCENTRATION PHENOMENA IN SEISMIC RESPONSE OF MULTISTORY FRAMES

K. UETANI and H. TAGAWA

Department of Architecture, Faculty of Engineering,
Kyoto University, Sakyo, Kyoto, Japan

ABSTRACT

An unknown type of collapse behavior is revealed for a multistory weak-beam planar frame subjected to a severe earthquake. This type of collapse behavior is characterized by deformation concentration in the restricted lower part of the frame. A method is proposed for the prediction of the height of the deformation concentration region. The validity of the method is verified through a numerical response analysis.

KEYWORDS

Multistory frame; collapse behavior; seismic response analysis; symmetry limit; bow-shaped mode; deformation concentration; weak-beam-type frames; earthquake-resistant design; deteriorating behavior; P-delta effect; elasto-plastic hysteretic behavior

INTRODUCTION

The senior author's symmetry limit analysis (Uetani 1992) has predicted that an unknown type of collapse behavior characterized by cyclic growth of a bow-shaped overall deflection mode could occur in the multistory multibay weak-beam planar frames subjected to a statically cyclic program of the top horizontal displacement, under a column axial force in excess of the symmetry limit (Uetani and Nakamura 1983). The weak-beam-type frames are generally believed to have superior earthquake resistance properties. But some further study of safety against severe earthquakes seems necessary, even with frames of this type, if such a bow-shaped mode could also appear and induce deformation concentration during an earthquake excitation.

In previous studies, numerical analyses of dynamic collapse behavior have been carried out for building frames in order to clarify their collapse properties (Tanabasi, Nakamura and Ishida 1974; Challa and Hall 1994; Ger, Chen and Lu 1993). However, theoretical studies for prediction of dynamic collapse behavior have not been performed. In this paper, deformation concentration phenomena in the process of dynamic collapse of strain-hardening and strain-softening frames of a weak-beam type are investigated. A theoretical method for the prediction of the height of the deformation concentration region (D.C. region) is proposed. The validity of the method is verified through a numerical response analysis, and properties of deformation concentration phenomena are clarified.

ANALYTICAL MODEL

Consider a fishbone-shaped subassemblage of the frame with s stories as shown in Fig.1. A lumped mass of m_i is allocated at the i -th story. This frame model is so designed that yielding may occur only at the beam ends and the bottom of the column in the first story as shown in Fig.2. Let the end moment-member rotation

angle relation of the beam in the i -th story (Fig.3(a)) obey a bi-linear rule as shown in Fig.4(a). The ratio of the stiffness after reaching the yield moment, M_{gi}^{p}, to the initial elastic stiffness is defined by α. Let the moment-rotation angle relation of a plastic hinge at the bottom of the column in the first story (Fig.3(b)) obey a bi-linear rule as shown in Fig.4(b). The yield moment is denoted by M_c^p, and the stiffness after reaching M_c^p is set to zero. For the i -th story, let EI_{gi} and EI_{ci} denote the elastic bending stiffness coefficient of beams and columns, respectively. Let $2l$ and r_i denote the length of all beams and the distance from base to centroid of the beam in the i -th story, respectively.

METHOD FOR PREDICTION OF THE HEIGHT OF THE D.C. REGION

A method for the prediction of the height of the deformation concentration region (D.C. region) in the case of the frame which consists of perfectly elastic-plastic members has been developed in previous studies (Uetani 1992; Uetani and Tagawa 1993; Uetani and Tagawa 1994a). This method may be summarized as follows. First, a subassemblage of the lower N stories with the height r_N is extracted from an original model as shown in Fig.5. Next, all the beams are removed, and a mass of $\sum_{i=N} m_i$, which represents the sum of masses above the N -th story, is placed at the top. Both the top and bottom ends of the long column are simply supported. The height, H^*, of the D.C. region can be determined from the following condition (Fig.6): if the long column of $N=N^*$ buckles under the mass weights, but the long column of $N=N^*-1$ does not, then $r_{N^*-1} < H^* < r_{N^*}$. The deformation concentration may occur in a particular mode, which coincides with the buckling deformation mode of the long column, if plastic hinges would be generated and operating at at least all the beam ends in the D.C. region and the bottom of the column in the first story.

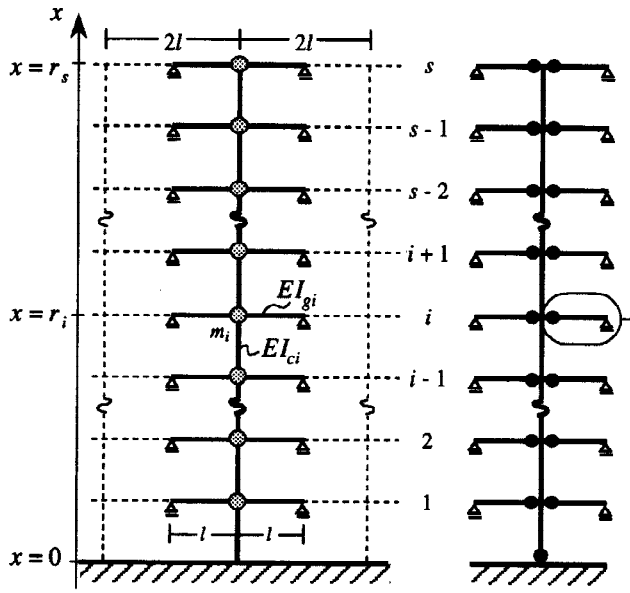

Fig.1 Analytical model

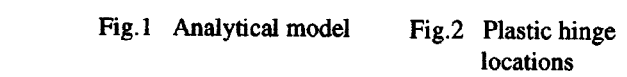

Fig.2 Plastic hinge locations

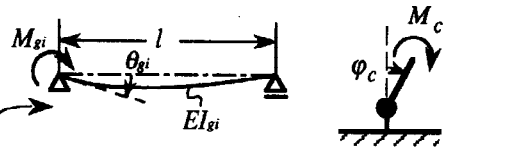

(a) Beam in the i -th story (b) Bottom of the column

Fig.3 Definition of moment and rotation angle

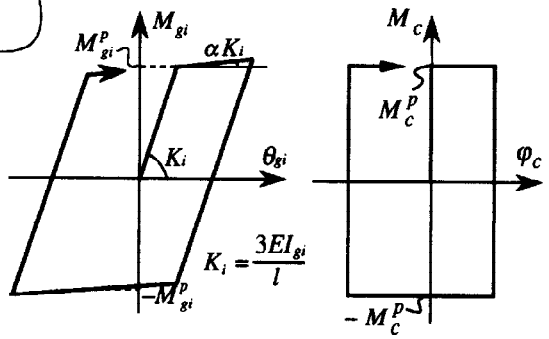

(a) Beam in the i -th story (b) Bottom of the column

Fig.4 Moment-rotation angle relationship

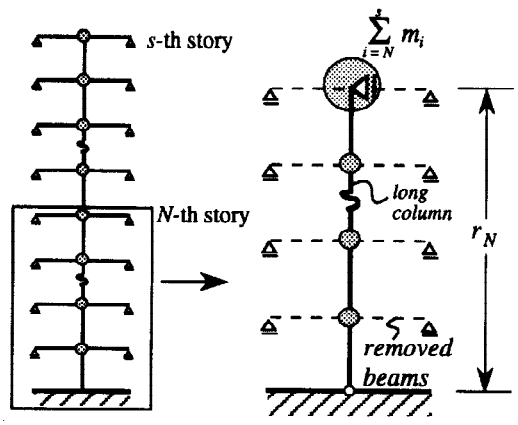

Fig.5 Subassemblage with N stories for prediction of the height of the D.C. region of perfectly elastic-plastic frames

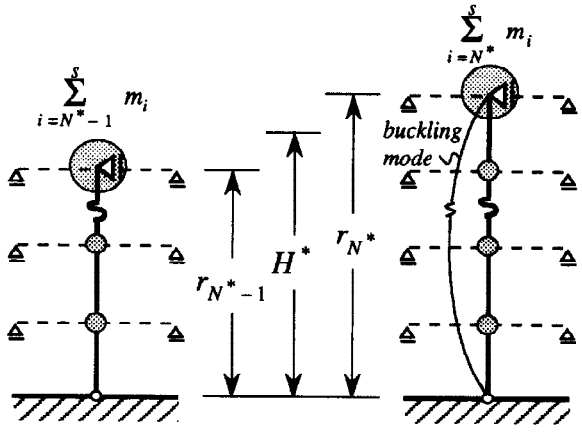

(a) Non-buckling (b) Buckling

Fig.6 Predicted height of the D.C. region ; H^*

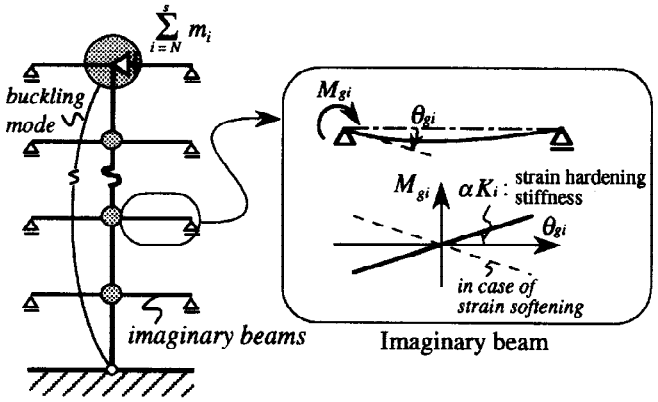

Fig.7 Subassemblage composed of columns and imaginary beams

Table-1 Dimensions of model frame

Number of stories	s	30
Height of i-th story	r_i	300 i (cm)
Span length	$2l$	600 (cm)
Lumped mass	m_i	40 (ton)

(1 ton = 1 kN sec^2/ m)

Table-2 Member properties

Story number i	Second moment of cross section ($\times 10^3$cm^4) Column I_{ci}	Beam I_{gi}	Yield moment of beam M_{gi}^p (tonf · cm)
1 ~ 5	400	160	16000
6 ~10	350	140	14000
11~15	300	120	12000
16~20	250	100	10000
21~25	200	80	8000
26~30	150	60	6000

(1tonf = 9.8 kN)

Table-3 Natural periods of the frame in the elastic range

1st	3.517 sec
2nd	1.287 sec
3rd	0.772 sec

Table-4 Relationship between N^* and stiffness ratio α

N^*	5	6	7	8	9	10
Ratio α	-0.106	-0.065	-0.036	-0.016	-0.002	0.007

Ratio α : the ratio of stiffness after yielding to the initial stiffness of beams

For a frame consisting of strain-hardening or strain-softening members, the method is to be modified as follows. Instead of removing beams from the subassemblage of N stories, the beams are replaced by imaginary elastic beams with strain-hardening or strain-softening stiffness representing the initial stiffness as shown in Fig.7. The height, H^*, of the D.C. region can be determined from the following condition : if the subassemblage of $N = N^*$ buckles under the mass weights, but that of $N = N^* - 1$ does not, then $r_{N^*-1} < H^* < r_{N^*}$.

NUMERICAL RESPONSE ANALYSIS

In this section, the accuracy and validity of the proposed method for the prediction of the height of the D.C. region, and the properties of deformation concentration phenomena are investigated through numerical response analyses of a 30-story frame model. Dimensions of the model frame are shown in Table-1. Member properties are shown in Table-2. The elastic modulus, E, is 2100 tonf/cm^2. Natural periods of the frame in the elastic range are shown in Table-3. The yield moment, M_c^p, at the bottom of the column in the first story is 30000 tonf · cm. The modal damping ratio, h_r, of the r-th mode is proportional to the natural frequency, and $h_1 = 0.02$. In the plastic range, the same damping ratios as those in the elastic range are used for each mode.

For this model, the relationship between the stiffness ratio, α, and the number of stories, N^*, contained in the D.C. region is shown in Table-4. The negative range of α is emphasized in this table, because clarification of the effects of deteriorating of member properties, due to local buckling, brittle fracture, etc., on frame behavior is one of the major purposes of this study. This table indicates that the height, H^*, of the D.C. region is bounded by $r_9 < H^* < r_{10}$ for $\alpha = 0$, by $r_5 < H^* < r_6$ for $\alpha = -0.1$, and so on.

In the computer program used here for a numerical response analysis, both material and geometrical non-linearities are taken into account to a reasonable extent for deriving reliable results (Uetani and Tagawa 1994b). By employing the total Lagrangean description and the conventional first-order non-linear approximation, a differential equation of lateral equilibrium is derived as follows:

$$EI_c\, v_{,xxxx}(x) + P v_{,xx}(x) = 0 \qquad (1)$$

where $v(x)$ is the column deflection; EI_c is the column bending stiffness coefficient; and P is the column constant axial force. $(\,)_{,x}$ represents the differential by x. The column stiffness matrices are calculated by using the general solution of equation (1).

Response Analysis to Impulsive Loading

Three different values of the stiffness ratio, α, are considered here. A comparatively large initial horizontal velocity of 300 cm/sec is applied to every mass. The column deformations at every 0.05 seconds are shown in Figs.8(a),(b),(c), respectively for $\alpha = 0, -0.04, -0.1$. A broken line in each figure indicates the predicted height of the D.C. region. A deformation concentration is observed in the columns just below the broken line for each case. Beam ductility factors are shown in Fig.9. In every case, a peculiar distribution is observed; beam ductilities are concentrated in the lowest several stories and the beam ductility of the first story is the largest. These distributions correspond to the deformation concentration. The beam ductility factor, μ_i, in the i-th story is defined by:

$$\mu_i = \frac{\left|\theta_{gi}^{max}\right|}{\theta_{gi}^{Y}} \qquad (2)$$

where θ_{gi}^{max} and θ_{gi}^{Y} denote the maximum value and yield point value of a beam-end rotation angle in the i-th story, respectively, $\theta_{gi}^{Y} = M_{gi}^{p}\, l / 3EI_{gi}$.

Seismic Response Analysis

The conditions of the seismic response analyses performed are listed in Table-5. The acceleration records of ground motion of El Centro NS 1940 and Taft EW 1952 are converted into the displacement expressions, which are used as input data. They have been scaled so that their maximum velocities are equal to 25, 50, 75, 100, 125, 150 cm/sec, respectively. Duration of ground motion is 20 seconds, but the analyses were terminated when the maximum horizontal displacement of any mass, relative to the ground, reached 200 cm.

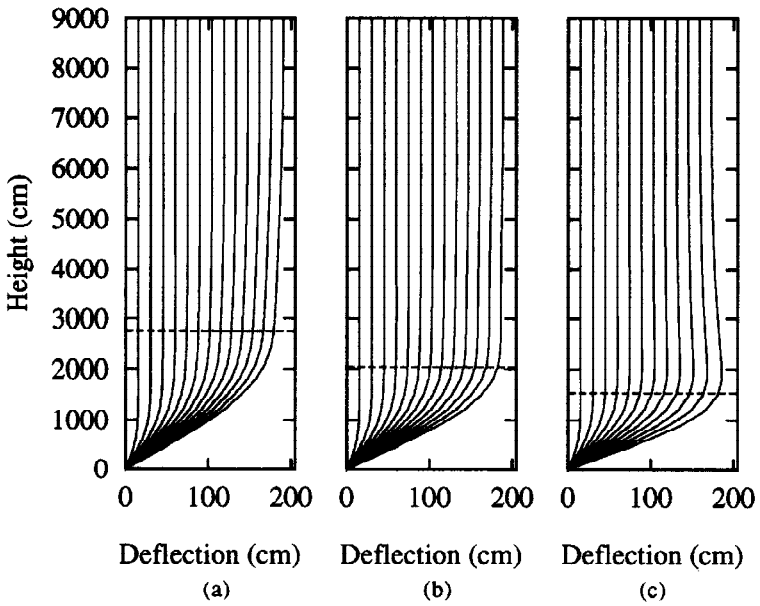

Fig.8 Results of response analysis to impulsive loading;
Column deformation, (a) $\alpha = 0$, (b) $\alpha = -0.04$, (c) $\alpha = -0.1$

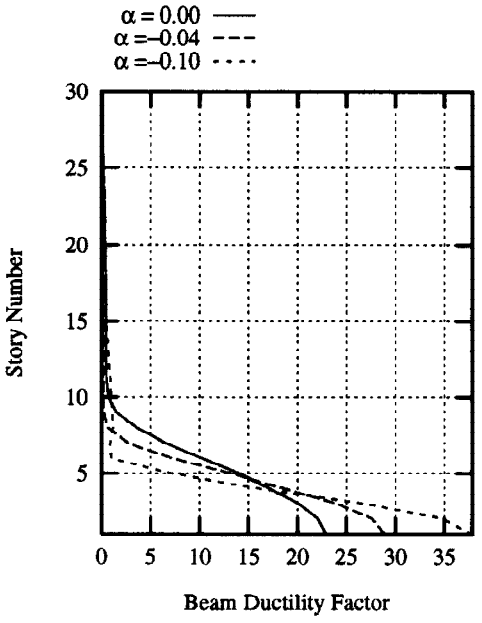

Fig.9 Beam ductility factors

Beam ductility factors are shown in Figs.10(a),(b),(c) and (d), respectively for the DE1, DE2, DE3 and DT1 series. In every case, peculiar distributions are observed under ground motions of Vmax=125 and 150 cm/sec. The distribution shapes coincide quite well with the results obtained from the response analyses to impulsive loading (Fig.9). In the case of DE3-75, the beam ductility factor peaks at the 9th story and remains small at the lowest five stories, because the bottom of the column in the first story does not yield. The D.C. region of this case is predicted in the next section.

Table-5 List of seismic responce analyses

Ground motion	Ratio α	Maximum velocity of ground motion (cm/sec)					
		25	50	75	100	125	150
El Centro NS	0	DE1-25	DE1-50	DE1-75	DE1-100	DE1-125	DE1-150
	- 0.04	DE2-25	DE2-50	DE2-75	DE2-100	DE2-125	DE2-150
	- 0.1	DE3-25	DE3-50	DE3-75	DE3-100	DE3-125	DE3-150
Taft EW	0	DT1-25	DT1-50	DT1-75	DT1-100	DT1-125	DT1-150

Ratio α : the ratio of stiffness after yielding to the initial stiffness of beams

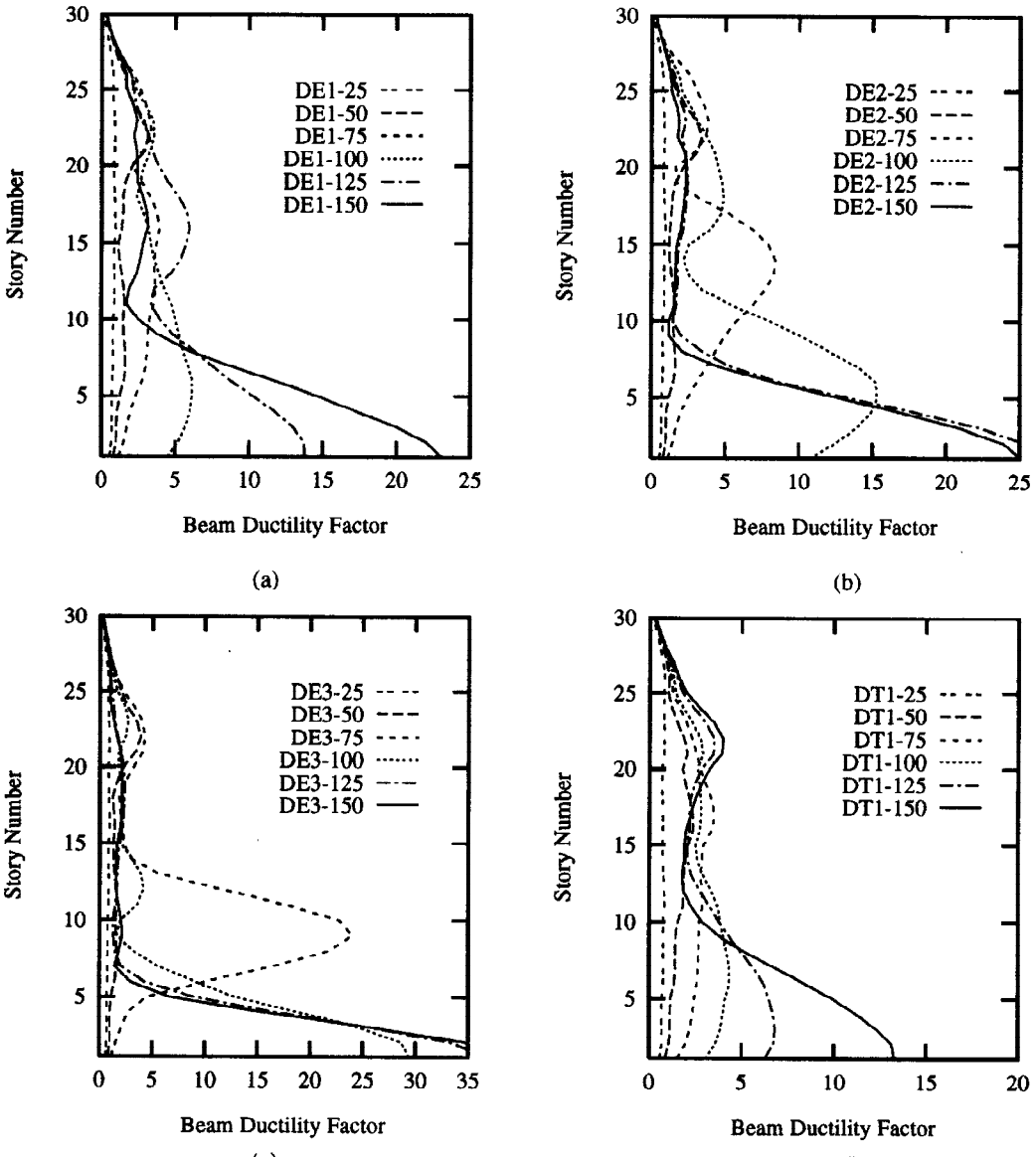

Fig.10 Results of seismic response analyses; Beam ductility factors,
(a) DE1 series, (b) DE2 series, (c) DE3 series, (d) DT1 series

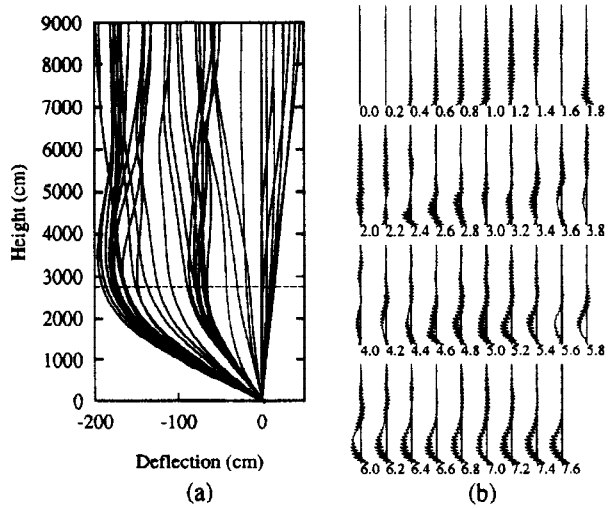

Fig.11 Results for DE1-150; (a)Column deformation, (b)Column bending moment

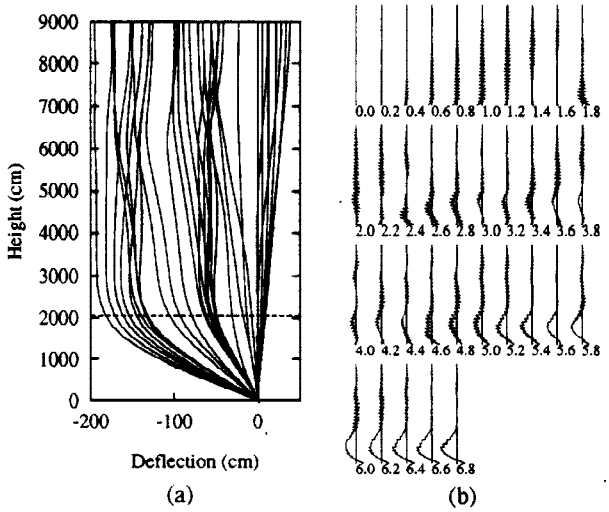

Fig.12 Results for DE2-125; (a)Column deformation, (b)Column bending moment

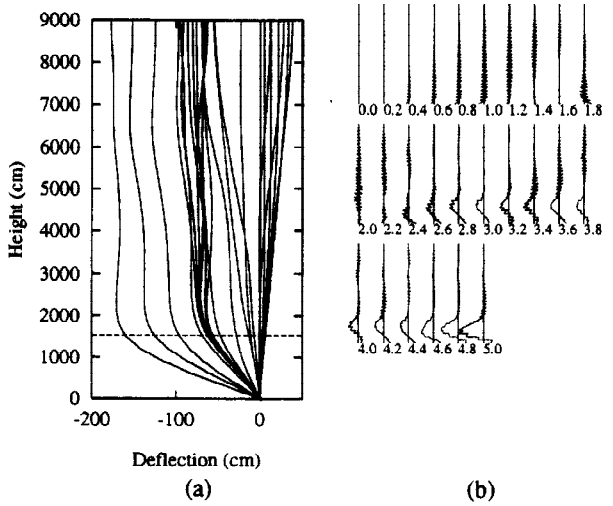

Fig.13 Results for DE3-125; (a)Column deformation, (b)Column bending moment

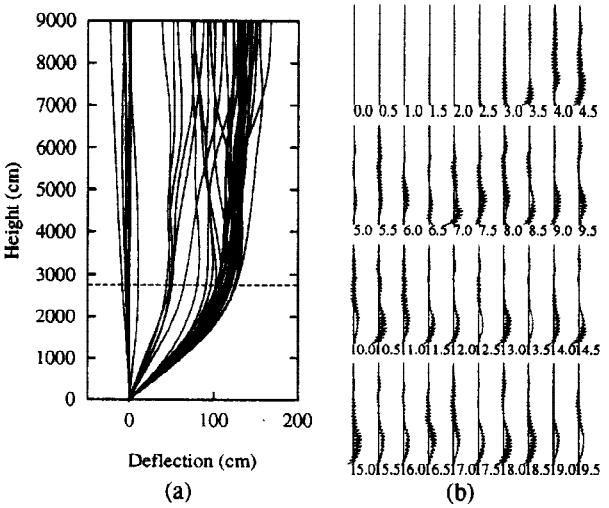

Fig.14 Results for DT1-150; (a)Column deformation, (b)Column bending moment

The numerical results for the cases of DE1-150, DE2-125, DE3-125 and DT1-150 are shown in Figs.11,12,13 and 14, respectively. Figures(a) show the horizontal displacements of the columns every 0.2 seconds (every 0.5 seconds in the case of DT1-150), and figures(b) show the distributions of the bending moments in the columns. In every case, the deformation concentration is observed in the lower portion as shown in figures(a). The number of the stories with a deformation concentration for $\alpha = -0.1$ is smaller than that for $\alpha = 0$. The deformation of the columns at the final stage are very similar to those observed in the response analyses to impulsive loading (Fig.8). A broken line in each figure indicates the predicted height of the D.C. region. Very good coincidence is observed between the deformation concentration region in the seismic response and the theoretical prediction in every case.

In every case, a bow-shaped distribution of the column bending moment appears in the lower part and its magnitude grows at the final stage as shown in figures(b). In these analyses, the columns, except for the bottom of the column in the first story, are assumed to remain elastic. If the elastic limit were also considered for the columns, the column bending moment would exceed this elastic limit, and a more sever collapse behavior would occur. It should be noted that the height of the D.C. region is very low for $\alpha = -0.1$, and the bow-shaped distribution grows very quickly.

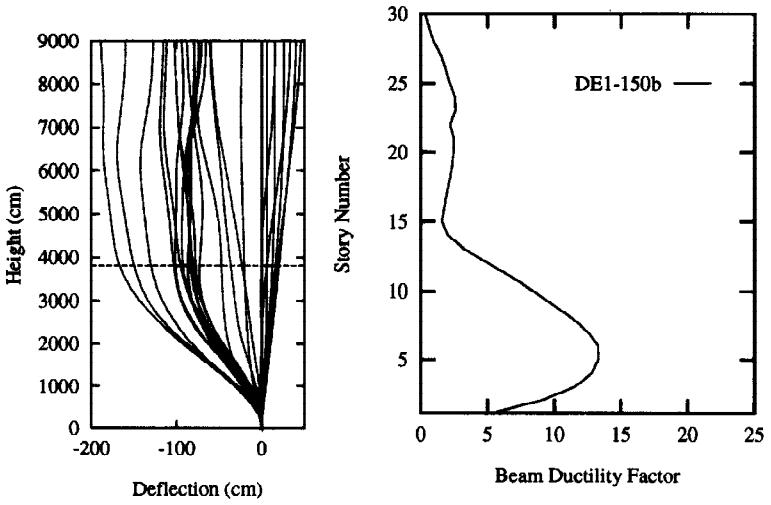

Fig.15 Results for DE1-150b; (a) Column deformation, (b) Beam ductility factor

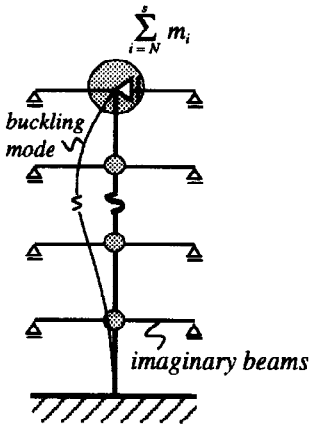

Fig.16 Subassemblage for prediction of the height of the D.C. region in the case of DE1-150b

Seismic Response Analysis in the case that the bottom of the column in the first story does not yield

For the analytical model in the last section, yielding of columns is allowed only at the bottom of the column in the first story. In this section, response analysis is performed for a model, whose columns are assumed to remain elastic everywhere. Analysis conditions are the same as the case of DE1-150, except that the yield moment, M_c^p, at the bottom of the column in the first story is set to infinity. This case is named DE1-150b.

The results of the response analysis of DE1-150b are shown in Fig.15. Figure(a) shows the horizontal displacements of the columns every 0.2 seconds. Figure(b) shows the beam ductility factor. A broken line in figure(a) indicates the predicted height of the D.C. region. The subassemblage used in this prediction is shown in Fig.16. The column in the first story is not simply supported, but fixed at the base. Good coincidence is observed between the deformation concentration region in the seismic response and the theoretical prediction. The D.C. region of DE1-150b is much larger than that of DE1-150. The beam ductility factor peaks at the 6th story as shown in figure(b).

CONCLUSIONS

An unknown type of dynamic collapse behavior of a multistory planar frame of a weak-beam type has been revealed through numerical response analyses. This type of behavior can be characterized by the growth of a bow-shaped deformation mode and the concentration of this mode in the restricted lower region of the frame. A theoretical method has been presented for prediction of the height of the deformation concentration region. It has been shown through the numerical response analyses that the deformation concentration region may be predicted by the proposed method with a good accuracy. The effects of the strain-hardening and strain-softening of beams on the collapse behavior have been also investigated.

It is broadly believed that the frames designed as to be of a weak-beam strong-column type would exhibit a stable and ductile hysteretic behavior under the action of strong earthquake and then have a desirable earthquake resistance property. In view of the results of this study, however, some further investigations of the deformation concentration phenomena seem to be necessary in order to propose some new design formula for rational resistance to the phenomena.

REFERENCES

Challa, V.R. Murty and John F. Hall (1994). Earthquake collapse analysis of steel frames, *Earthquake Engineering and Structural Dynamics*, **23**, 1199-1218.

Ger, J. F., F. Y. Cheng and L.W. Lu (1993). Collapse behavior of Pino Suarez Building during 1985 Mexico City Earthquake, *J. Struct. Engrg.*, ASCE , **119 (3)**, 852-870.

Tanabashi, R., T. Nakamura and S. Ishida (1974). Gravity Effect on the Catastrophic Dynamic Response of Strain-Hardening Multi-story Frames, *Proc. of the Fifth World Conference on Earthquake Engineering*, Roma, Italy, **2**, 2140 - 2151.

Uetani, K. (1992). Cyclic plastic collapse of steel planar frames. In: *Stability and Ductility of Steel Structures under Cyclic Loading* (Y. Fukumoto and G. Lee, Ed.), CRC press, 261-271.

Uetani, K. and T. Nakamura (1983). Symmetry limit theory for cantilever beam-columns subjected to cyclic reversed bending, *Journal of the Mechanics and Physics of Solids*, **31 (6)**, 449-484.

Uetani, K. and H. Tagawa (1993), Bifurcation behavior analysis of multistory planar frame model subjected to one-way top horizontal displacement, *Journal of Struct. Constr. Eng.*, AIJ, **453**, 101-110. (in Japanese)

Uetani, K. and H. Tagawa (1994a), Dynamic collapse of weak-beam-type planar frames, *Proc. of Annual Meeting*, AIJ, 1313-1316. (in Japanese)

Uetani, K. and H. Tagawa (1994b), Dynamic collapse behavior analysis of multistory multibay planar frames, *Proc. of the Third World Congress on Computational Mechanics*, **1**, 147-148.